Subsidence Impact Analysis — Sensitivity Study

Addendum to Itasca Report "Assessment of Surface Subsidence Associated with Caving — Resolution Copper Mine Plan of Operations"

ITASCA
Consulting Group, Inc.

Subsidence Impact Analysis – Sensitivity Study

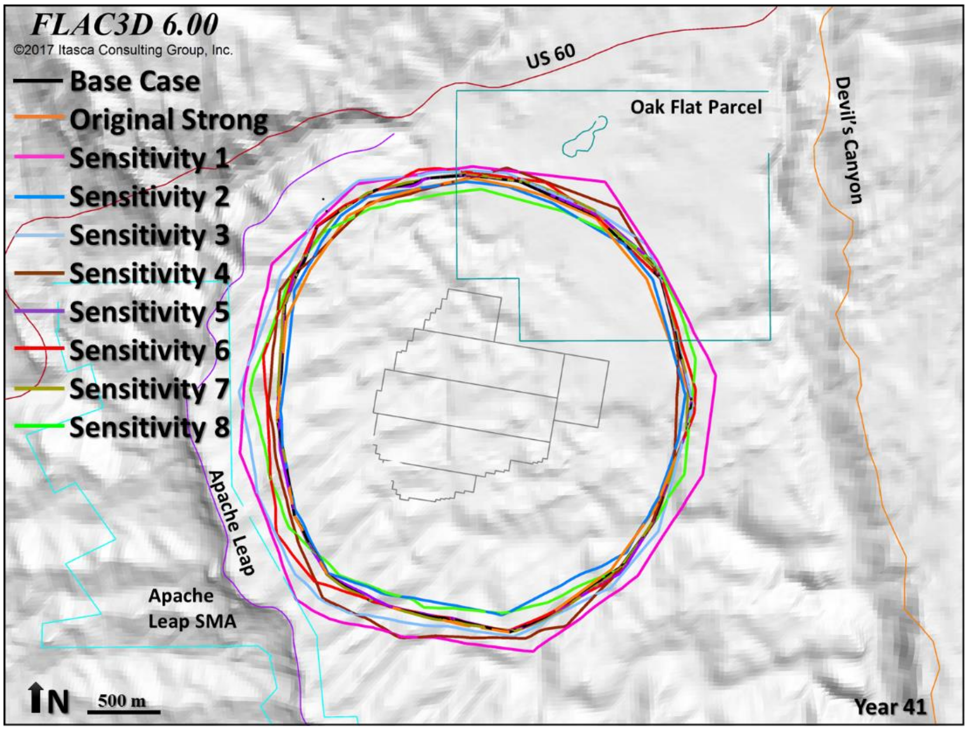

Prepared For:
Resolution Copper Mining LLC

April 6, 2018
Ref. 2-5605-01:18R10

Prepared By:
Tryana Garza-Cruz,
Itasca Consulting Group, Inc.
Matthew Pierce,
Pierce Engineering

ITASCA
Consulting Group, Inc.

111 Third Ave South, Suite 450
Minneapolis, MN 55401
phone: 1 612 371-4711 fax: 1 612 371-4711
email: icg@itascacg.com
web: www.itascacg.com

Table of Contents

1.0 INTRODUCTION

In 2017, Itasca conducted geomechanical studies of cave growth and subsidence potential for Resolution Copper Mining. The results of these studies are documented in a report titled "Assessment of Surface Subsidence Associated with Caving Resolution Copper Mine Plan of Operations" (referred to in this document as Surface Subsidence report). A subsidence impact model was run to support the mine plan of operations, which was submitted to the United States Forest Service (USFS) in November 2013 to initiate the comprehensive environmental review under the National Environmental Policy Act (NEPA) with the completion of an Environmental Impact Statement (EIS). The main purpose of the study was to evaluate the potential ground collapse and surface deformations associated with caving at Resolution Copper for the Environmental Impact Study (EIS) based on a production schedule of approximately 135,000 short tons per day (120,000 metric tonnes per day). The analyses were conducted using industry standard methods (*FLAC3D*) and employed independent laboratory-derived rock mass properties and fault geometry data collected by Resolution engineering staff and subsequently reviewed by third-party Competent Persons (CP). Conservative strength estimates were derived for the faults by Itasca and Resolution based on the mapped/logged geologic character of the faults and then subsequently downgrading the strength relative to the surrounding rock mass. The results of the study suggest a variable cave angle around the footprint perimeter, ranging from 70–78° by the end of mine life. The steep cave angles are a result of the deep footprint location and blind nature of the orebody (waste cap is present directly above the orebody). In all cases examined, no damage to the Apache Leap, Devil's Canyon or to the serviceability of Highway US-60 was predicted.

After reviewing the results, a sensitivity analysis was commissioned to understand the impact of a number of model input parameters on the predicted subsidence limits. This document is presented as an addendum to the original report, documenting the results of this sensitivity analysis.

Additionally, the slides of the presentation to the US Forest Service on March 16th, 2018 are included in Appendix A for reference.

2.0 SENSITIVITY ANALYSIS

The main factor driving the size and lateral extent of subsidence is the depth and footprint of the ore body to be mined. However, there are other factors associated with the geotechnical properties of the rock and structures that may also have an effect on the shape of subsidence, in particular the area of disturbance or fracture zone. Table 1 outlines the base case (MPO Surface Subsidence) and sensitivity analysis conducted, which examined rock mass strength, fault strength, caved rock porosity and in-situ stresses. The basis and results for each parameter variation are described in more detail in the following subsections. In all cases, the fracture zone limits are plotted to illustrate the model sensitivity. The fractured zone is defined by a region with the total measure of strain exceeding 0.5% and it represents the expected limits of visible fracturing on the ground surface.

Table 1 Summary of Sensitivity Analyses Conducted

Model name	Rock Mass Strength		Fault Strength	Maximum Caved Rock Porosity	In Situ Stress	
	Peak Strength	Residual Strength			K0 Values	sH Orientation
Base Case	100%	Base Case	Base Case	40%	Base Case	N-S
Original Strong	100%	Base Case	**Strong Case**	40%	Base Case	N-S
Sensitivity 1	**75%** σ_{cm}	Base Case	Base Case	40%	Base Case	N-S
Sensitivity 2	**125%** σ_{cm}	Base Case	Base Case	40%	Base Case	N-S
Sensitivity 3	100%	Base Case	**Weak Case**	40%	Base Case	N-S
Sensitivity 4	100%	**Sensitivity**	Base Case	40%	Base Case	N-S
Sensitivity 5	100%	Base Case	Base Case	**30%**	Base Case	N-S
Sensitivity 6	100%	Base Case	Base Case	40%	**125%**	N-S
Sensitivity 7	100%	Base Case	Base Case	40%	**75%**	N-S
Sensitivity 8	100%	Base Case	Base Case	40%	Base Case	**E-W**

2.1 Rock Mass Strength

The derivation of peak and residual rock mass strengths from the intact and rock mass data provided by Resolution is described in Section 4.3 of the Surface Subsidence report. The sensitivity to each of these inputs was investigated in turn.

2.1.1 Peak Strength

Table 2 summarizes the global rock mass strength (σ_{cm}) values used for the base case analysis and the two sensitivity analyses reported here (weaker and stronger than the base case). σ_{cm} can be estimated from the intact strength, σ_{ci}, and Hoek Brown *m*, *s* and *a* parameters (outlined in Table 3 of the Surface Subsidence report) using the following relations from Hoek et al. (2002):

$$\sigma'_{cm} = \sigma_{ci} \frac{\left(m_b + 4s - a\left(m_b - 8s\right)\right)\left(m_b / 4 + s\right)^{a-1}}{2\left(1+a\right)\left(2+a\right)}$$

Since fault strengths are always expressed as a percentage of host strength, these are also scaled with the peak rock mass strength sensitivity analyses (i.e., both the unit strengths and fault strengths are raised or lowered in the sensitivity analysis of global rock mass strength).

Comparison of the base case and sensitivity fracture limits (Figure 1) shows that the reduction in fracture limit is marginal for the stronger case, indicating that at the base case strengths, the fracture limit is most strongly controlled by the footprint depth and geometry. The weaker case, on the other hand, increases the potential for yielding at shallow levels (less confinement) so the cave angle becomes shallower in the near surface, extending in all directions but more strongly to the southwest.

Table 2 Rock Mass Peak Strength Base Case and Sensitivity Cases (expressed in MPa)

Unit	Base Case	Sensitivity Study	
	Rock Mass Global Strength, σ_{cm}	75% σ_{cm}	125% σ_{cm}
Diabase, Basalt	11.3	8.5	14.1
Diabase with anhydrite	29.4	22.0	36.7
Breccia, QEP	12.8	9.6	16.1
Quartzite	38.4	28.8	48.0
Tal (Apache Leap Tuff)	25.9	19.5	32.4
Tw (Whitetail)	9.5	7.2	11.9
KVS, KQS	18.8	14.1	23.5
Skarn	19.7	14.7	24.6

In order to test the conservativeness of the lower strength sensitivity, a Monte Carlo analysis of Apache Leap rock mass global strengths was carried out. Monte Carlo is a well-established technique for understanding rock mass strength distribution that involves randomly sampling the input distributions of GSI, UCS, and m_i to calculate a distribution of rock mass strength from the Hoek-Brown criterion (e.g., see Li et al., 2012; Sari et al., 2010). The input distributions for UCS (227 samples, Figure 2) and GSI (302 samples, Figure 3) were derived from the point load derived UCS and Joint Weighted Density (JWD) derived GSI statistics provided by Resolution, while the statistically derived m_i value was fixed at 25. As noted in Figure 2, the UCS values were scaled by a factor of 0.8 to account for the drop in intact strength expected when moving from lab-scale to cave-scale (Hoek and Brown, 1980). The distribution in Apache Leap Tuff global strength resulting from 5000 random samples of these inputs gives the distribution shown in Figure 4. The base case global strength of 26 MPa corresponds to the 27th percentile strength. This is close (and more conservative) to the 30th percentile strength typically employed in cave-scale simulations (e.g., see Pierce, 2010; Rafiei Renani et al., 2018). The lower strength sensitivity strength of 19.6 MPa, on the other hand, corresponds to the 15th percentile strength, which represents a very conservative assumption. **Thus, the fracture limits corresponding to this lower strength sensitivity are considered highly unlikely**.

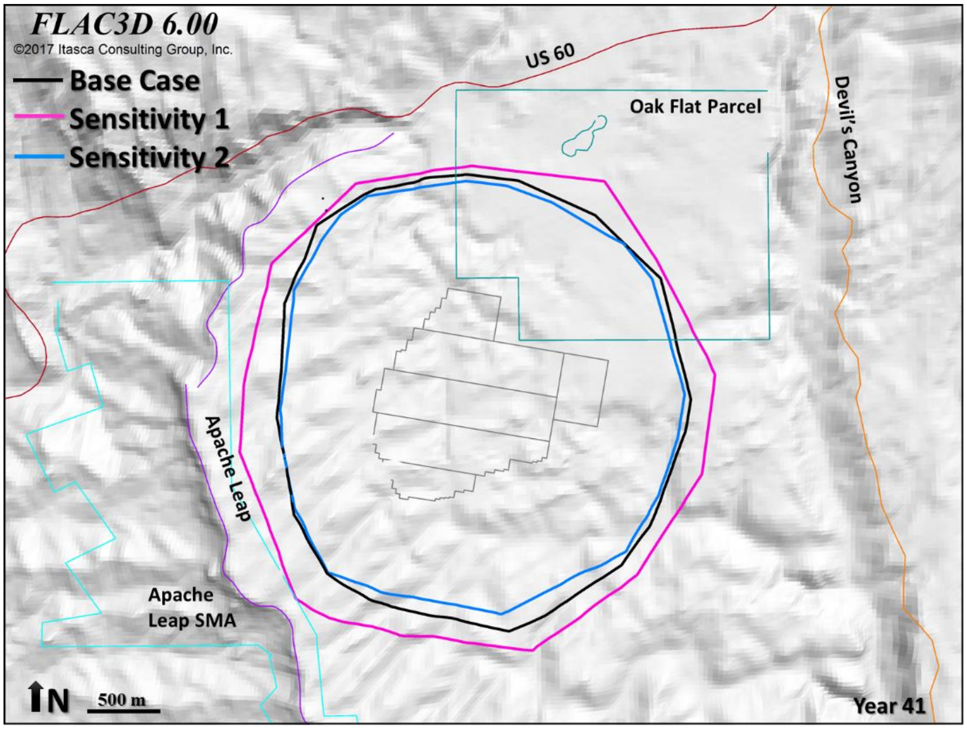

Figure 1 Comparison of predicted fracture limits for base case global rock mass strengths (black line) relative to a stronger case (+25%, Sensitivity 2, blue line) and a weaker case (-25%, Sensitivity 1, magenta line).

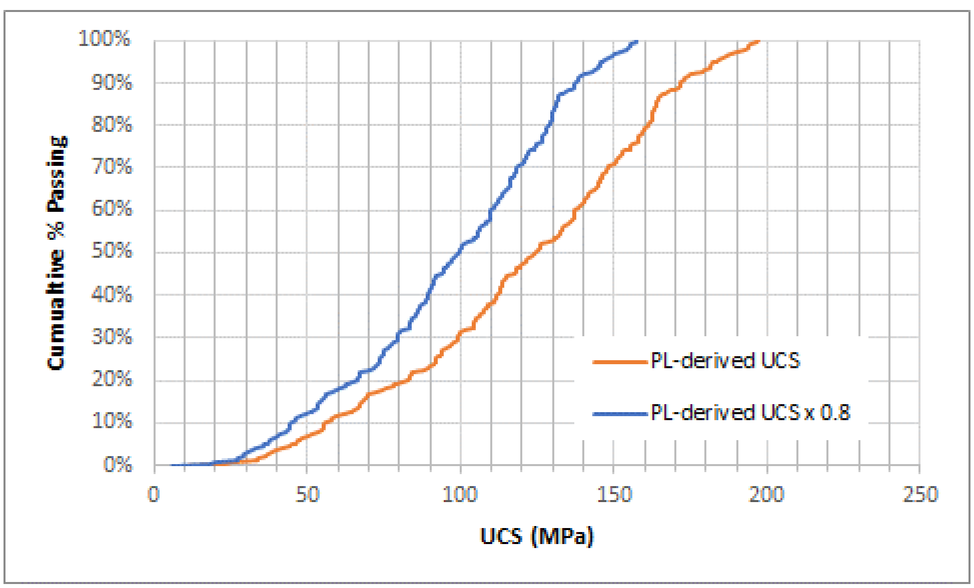

Figure 2 Distribution in point load derived UCS for the Apache Leap Tuff with size effect scaling shown.

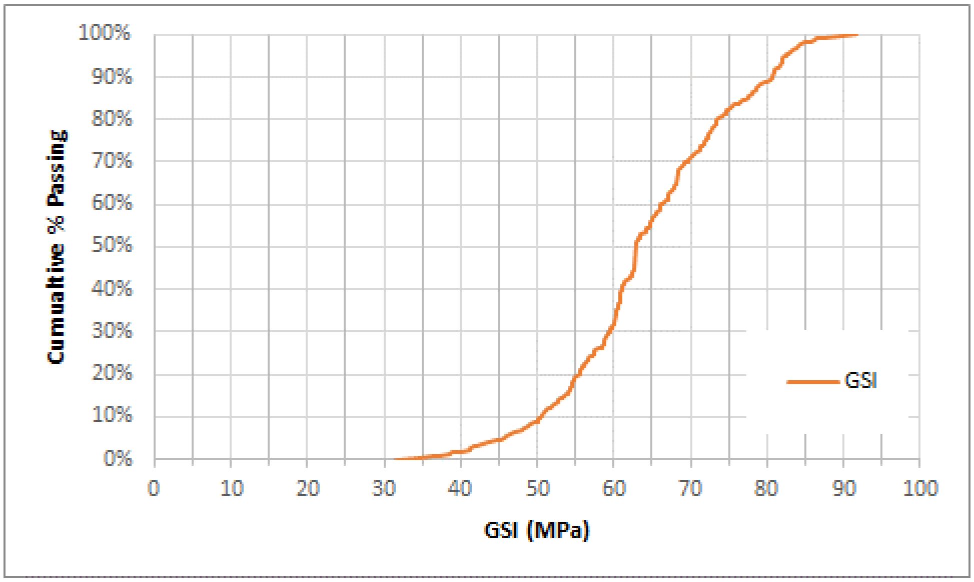

Figure 3 ***Distribution in Joint Weighted Density (JWD) derived GSI for the Apache Leap Tuff with size effect scaling shown.***

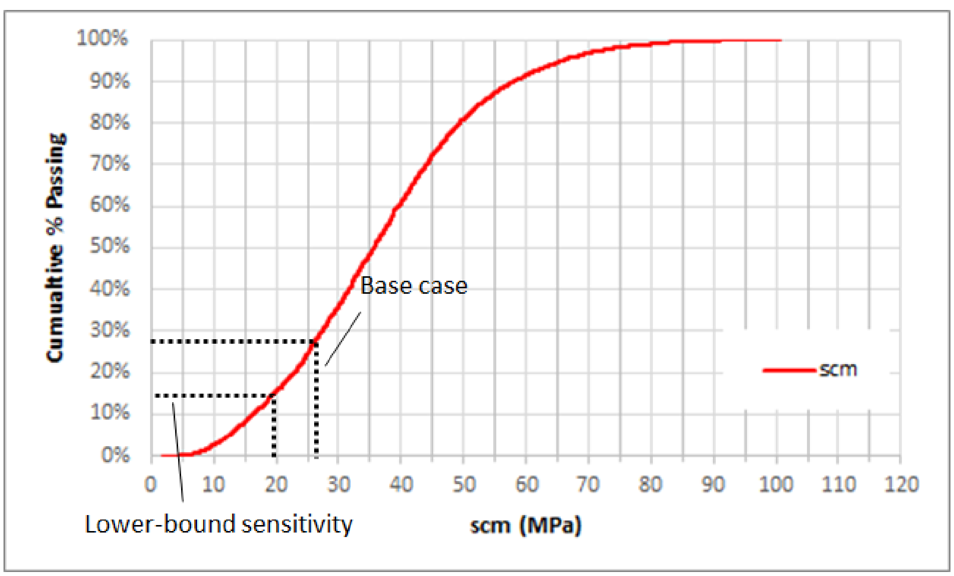

Figure 4 ***Distribution in Apache Leap global rock mass strength derived from Monte Carlo analysis. Base case and lower strength sensitivities indicated.***

2.1.2 Residual Strength

Figure 5 shows the base and sensitivity cases examined for residual strength, and Figure 6 compares the fracture limits for the two cases. The main impact of lowering the residual strength is to encourage more shear localization, which makes the fracture limit more chaotic. The end result is a fracture limit that becomes more extended in some areas and restricted in others but is not dramatically impacted overall.

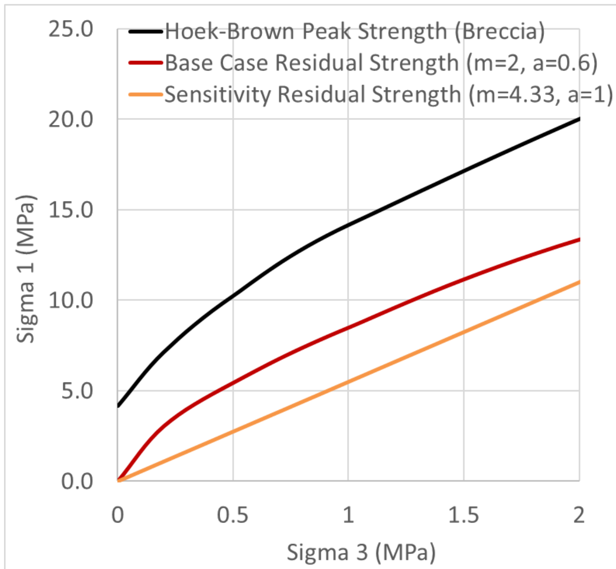

Figure 5 Rock mass residual strength base case (red curve) and sensitivity case (lower orange curve equivalent to zero cohesion and 43° friction angle). Peak strength of Breccia unit shown for comparison.

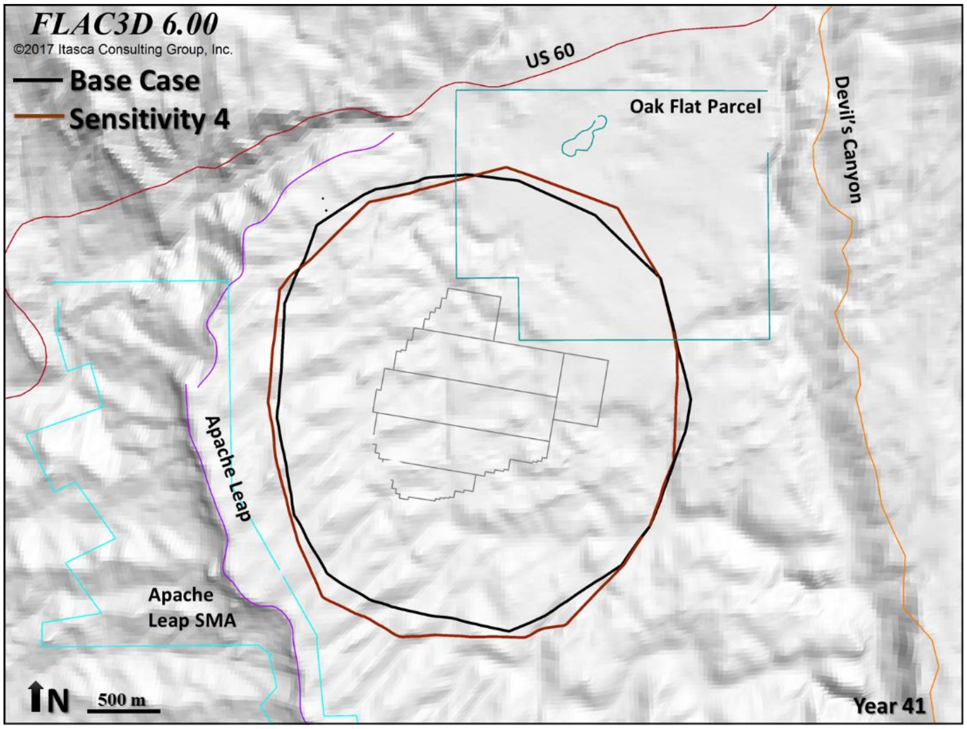

Figure 6 Comparison of predicted fracture limits for base case rock mass residual strength (black line) relative to a weaker case (Sensitivity 4, brown line).

2.2 Fault Strength

The categorization of faults into strong, medium, or weak and the estimated strength properties is described in Section 4.2 of the Surface Subsidence report. Table 3 summarizes the strengths used for the different categories and sensitivities. It is important to note for the medium and strong cases, that the fault is weakened relative to its host rock unit by a percentage of the host global rock mass strength. **The level of conservatism with respect to fault representation and strength is high in all cases** examined (even the base case) due to the following:

- Strong faults at Resolution exhibit an annealed character which (in many cases) makes them stronger than the surrounding rock mass. In all cases examined, they are assumed to be weaker to some degree.
- Faults have been assumed to be fully persistent.
- Due to the challenges associated with fault strength characterization, weak faults have been assigned a low friction angle with zero cohesion, which precludes the existence of any offsets or asperities on the fault surface.

Figure 7 shows that fault strengths do not impact fracture limits significantly, except in the southwest where lower strength faults tend to pull the fracture limit out. This is a result of the Gant fault present in that locale (see Figure 8).

Table 3: Fault strength base case and sensitivity cases

	Base Case	Sensitivity Study	
		Higher Strength	Lower Strength
Strong Faults	75% σ_{cm}	88% σ_{cm}	50% σ_{cm}
Medium Faults	50% σ_{cm}	72% σ_{cm}	25% σ_{cm}
Weak Faults	cohesion = 0 tensile strength = 0 friction = 35°	cohesion = 0 tensile strength = 0 friction = 35°	cohesion = 0 tensile strength = 0 friction = 25°

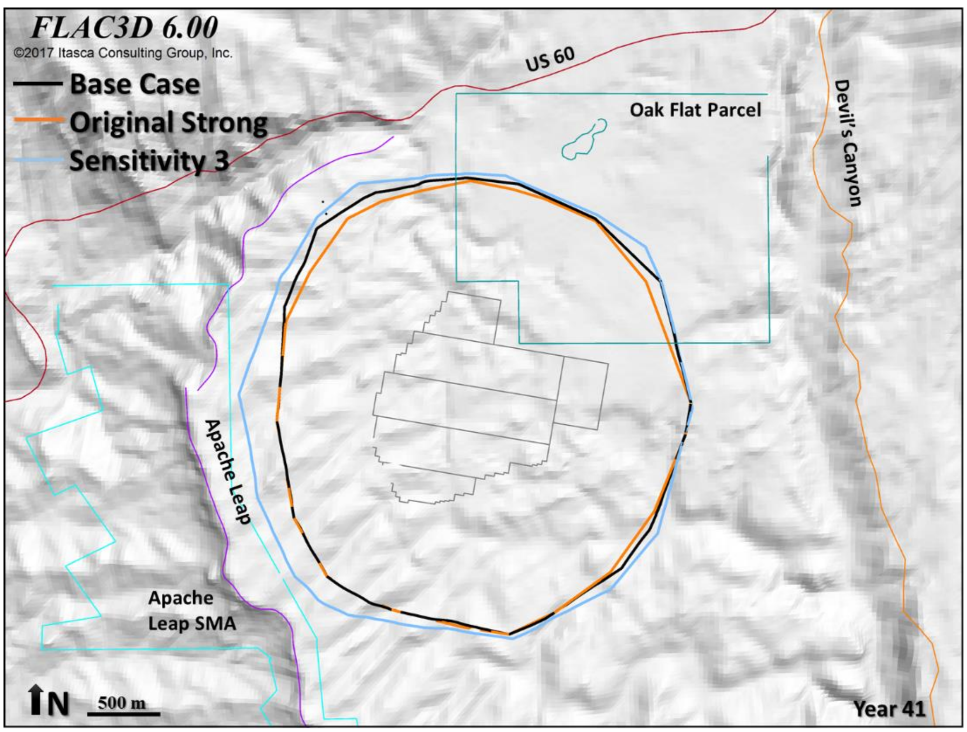

Figure 6 ***Comparison of predicted fracture limits for base case fault strengths (black line) relative to a weaker case (Sensitivity 3, blue line) and a stronger case (Original Strong, orange line).***

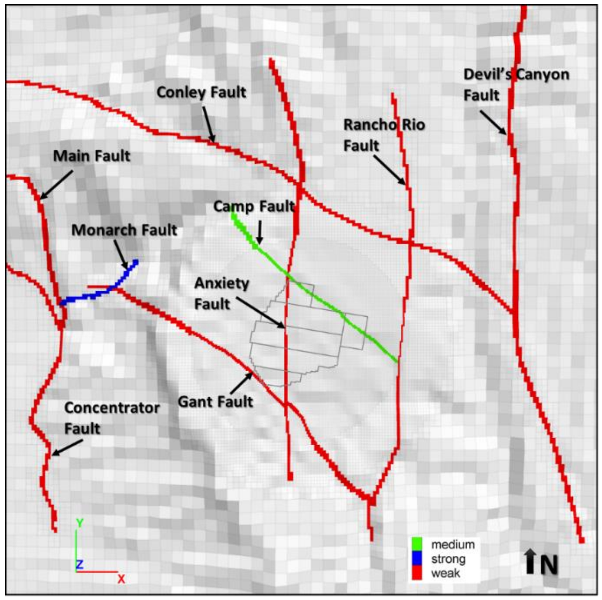

Figure 7 Location of faults at ground surface. Note Gant fault located to the southwest, which impacts fracture limits there when weakened sufficiently.

2.3 Caved Rock Maximum Porosity

The maximum caved rock porosity of 40% used for the base case analyses is discussed in more detail in Appendix 1, Section 1.6.1 of the Surface Subsidence report. A lower value of 30% was examined for the sensitivity analysis. As shown in Figure 8, the reduction in maximum porosity from 40% to 30% does not impact the predicted fracture limits. This is due to the low overall porosity of the Resolution cave for the interactive draw conditions represented. The average cave porosity is predicted to increase gradually from 10.2% at Year 5 to 13.6% at year 41. This corresponds well with the average cave porosities commonly reported for caving mines (see Table 4).

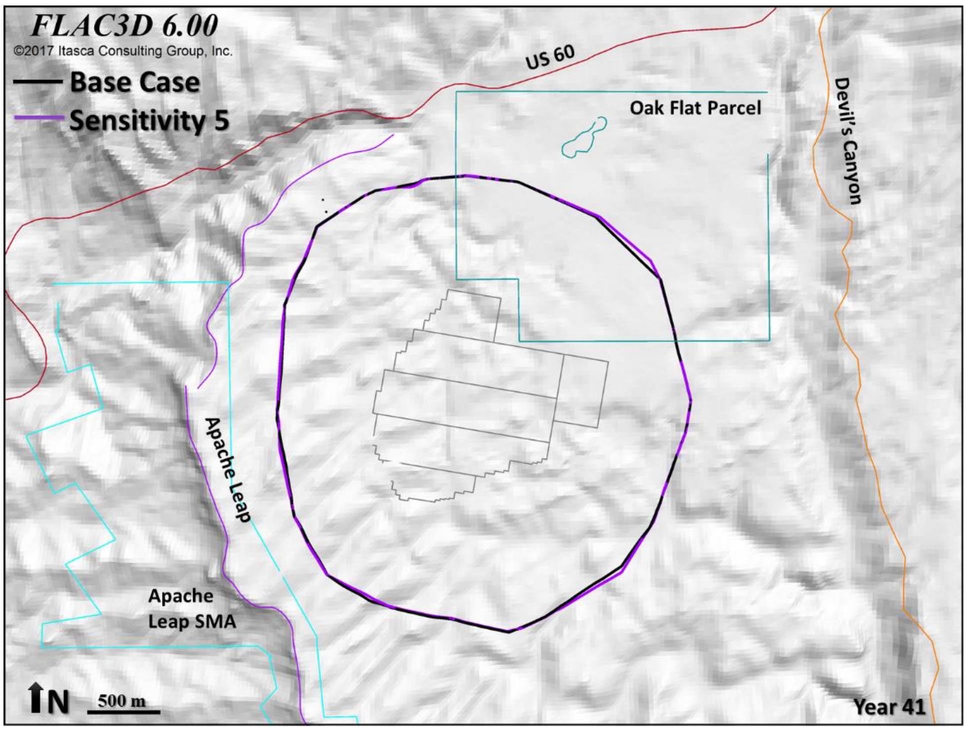

Figure 8 ***Comparison of predicted fracture limits for base case maximum caved rock porosity (40%, black line) relative to a lower porosity (30%, Sensitivity 5, purple line).***

Table 4 Summary of Block Caving Mines and Cave Parameters (after Sharrock et al. 2009)

Mine	Block	Swell (%)	Fragmentation P = primary (> $2m^3$) S = secondary (< $2m^3$) D = draw rate PR = propagation rate M = max. block size	Geometry HR = hydraulic radius D = depth C = column height	Rockmass conditions
Northparkes	E26 Lift 1	Muckpile: 120 (14) Collapse: 110 (14)	P: 25% S: 10% D: 110 to 380 mm/day	HR: 38m D: 480m	RMR: 23 to 53 (6) Q: 8.73
Ridgeway	Ridgeway Deeps	110 (15)			
Henderson		109.5 (2)	PR: 0.70 m/day		
Lakeshore		109.5 (4)	PR: 1.98 m/day		
Questa	Goat Hill	109.0 to 121.0 (10)		H: 28m D: 300m C: 90m-200m	Q: 0.002 to 8
	Questa D Block 1	110 (10)	PR: 0.6 m/day	H: 28m	Q: 0.002 to 8
San Manuel	South	109 (1)	PR: 0.49 m/day		
	All	130 (1)			
Andina	Panel I & II	120 (12)		H: 23m (7)	Q: 0.4 MRMR: 44 (7)
	Panel III	115 (12)			
El Teniente	Esmeralda	136 (8)			
		119 (14)			
		128 (14)			
Freeport	DOZ	115 (13)	Diorite P: 80 M: 2m		RMR: 55 to 65
Palabora		120 (11)			
King		113 (5)		H: 18m (9)	MRMR: 30 (9)

References
(1) Johnson & Soule (1963)
(2) Brumleve & Maier (1981)
(3) Heslop (1984)
(4) Panek (1984)
(5) Brumleve (1987)
(6) Van As & Jeffrey (2000)
(7) Mawdesley (2002)
(8) Leiva, & Duran (2003)
(9) Brown (2004)
(10) Gilbride et al. (2005)
(11) Moss et al. (2006)
(12) Alcalde et al. (2008)
(13) Pasetyo (pers. comm 2008)
(14) ICS report
(15) Sharrock (2012)

2.4 In-situ Stress

The stress regime used for the base case analysis is based on hydrofracturing tests done on site and is described in Section 4.4 of the Surface Subsidence report. The sensitivity to in-situ horizontal stress magnitude and orientation was investigated in turn.

2.4.1 Ratio of Horizontal to Vertical Stresses (K_0)

The K_0 value (ratio of horizontal to vertical stresses) was both raised and lowered in the sensitivity analyses (see Table 5). As shown in Figure 9, the stress magnitude has a minimal impact on the fracture limits. This is due to the fact that there are no locked-in stresses at surface at Resolution, so the difference in stress regime is not significant in the near-surface.

Table 5 In-situ Stress Base Case and Sensitivity Cases

	Base Case	Sensitivity Study	
Principal Stress	Magnitude	75% K_0	125% K_0
σ_V	25.5*z [km]	25.5*z [km]	25.5*z [km]
σ_H	20.4*z [km]	15.3*z [km]	25.5*z [km]
σ_h	12.75*z [km]	9.56*z [km]	15.94*z [km]

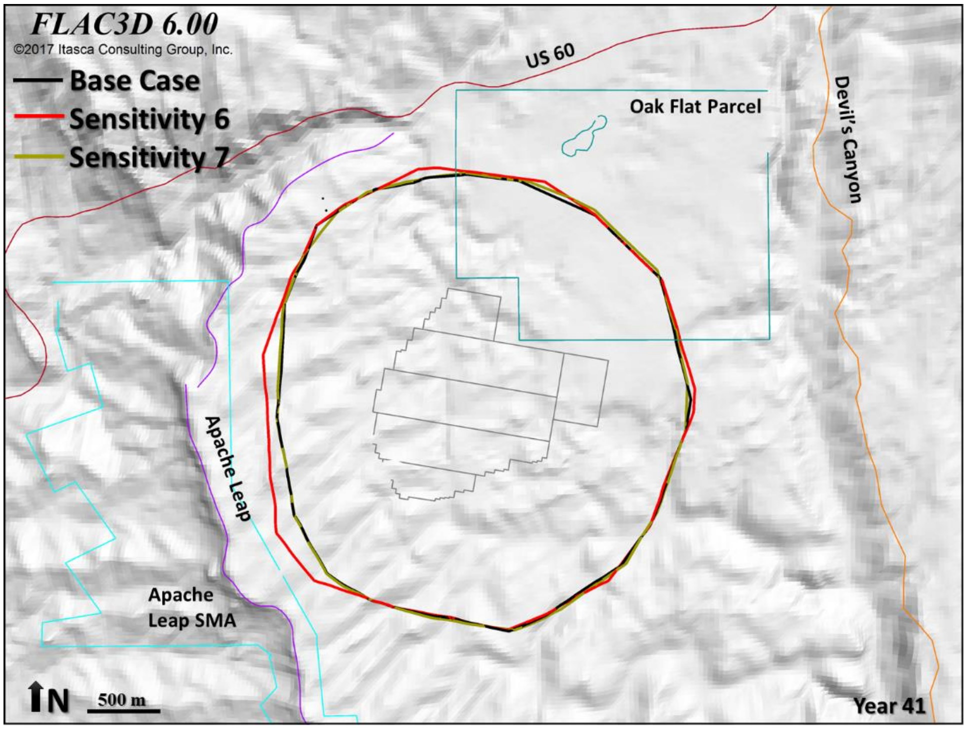

Figure 9 Comparison of predicted fracture limits for base case in-situ stress magnitude (black line) relative to lower horizontal stresses (K_0-25%, Sensitivity 6, red line) and higher horizontal stresses (K_0+25%, Sensitivity 7, olive line).

2.4.2 Orientation of Horizontal Principal Stresses

The orientation of the major horizontal principal stress was rotated 90 degrees in another sensitivity run (keeping the base case magnitudes as measured). As expected, the rotation of the direction of in-situ stress rotated the long axis of the fracture limits from N-S to E-W (Figure 10).

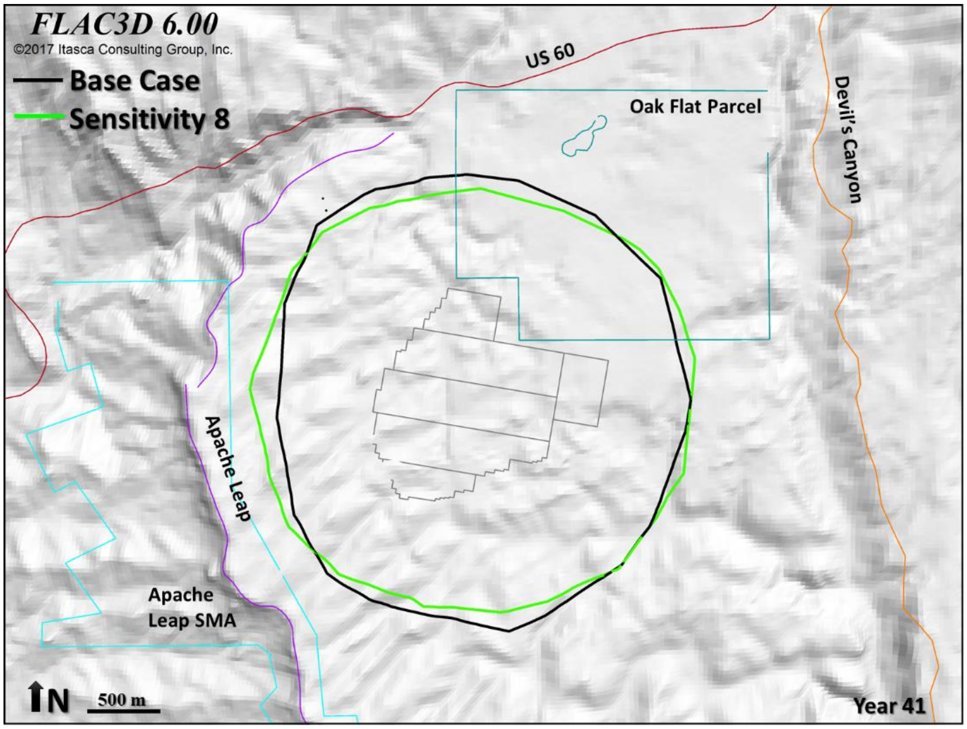

Figure 10 Comparison of predicted fracture limits for base case orientation of major horizontal principal stress (N-S, black line) relative to a 90° rotation (E-W, Sensitivity 8, green line).

3.0 DISCUSSION AND CONCLUSIONS

Figure 11 shows the results of the base case fracture limits at end of mine life compared to all the sensitivity runs carried out. The analyses suggested the following sensitivities:

- Weaker rock mass global strengths (-25%) extend the fracture limit in all directions.
- A lower rock mass residual strength slightly reduces the fracture limit in some locations and slightly extends it in others.
- Lower fault strengths extend the fracture limit to the southwest, due to the location and orientation of the Gant fault located there.
- A lower maximum caved rock porosity does not affect the fracture limit for the interactive draw simulated.
- A higher in-situ horizontal stress magnitude (K0 + 25%) extends the fracture limit slightly to the southwest.
- A 90° rotation in horizontal in-situ stresses causes a rotation of the long axis of the fracture limit to an East-West direction.

Table 6 summarizes the differences in breakthrough timing maximum crater depth at the end of mine life for the cases examined. The results suggest minimal variability in cave breakthrough timing with Year 6-7 being observed in all cases. The crater depths are consistently between 240-280 m, with the exception of the stronger fault sensitivity, in which the crater depth is greater due to the restriction of the cave limit on the east side. This is due to the Camp Fault, which acts to limit the cave boundary relative to the base case when strengthened (Figure 12).

In general, the fracture limits at Resolution are most strongly controlled by the extraction level depth and shape (with deeper caves like Resolution having steeper cave angles than shallow caves) and the blind nature of the orebody (with deep orebodies with a waste cap like Resolution resulting in less subsidence than orebodies for which the entire column is ore to be drawn out). In all cases examined, no damage to the Apache Leap, Devil's Canyon or to the serviceability of Highway US-60 was predicted.

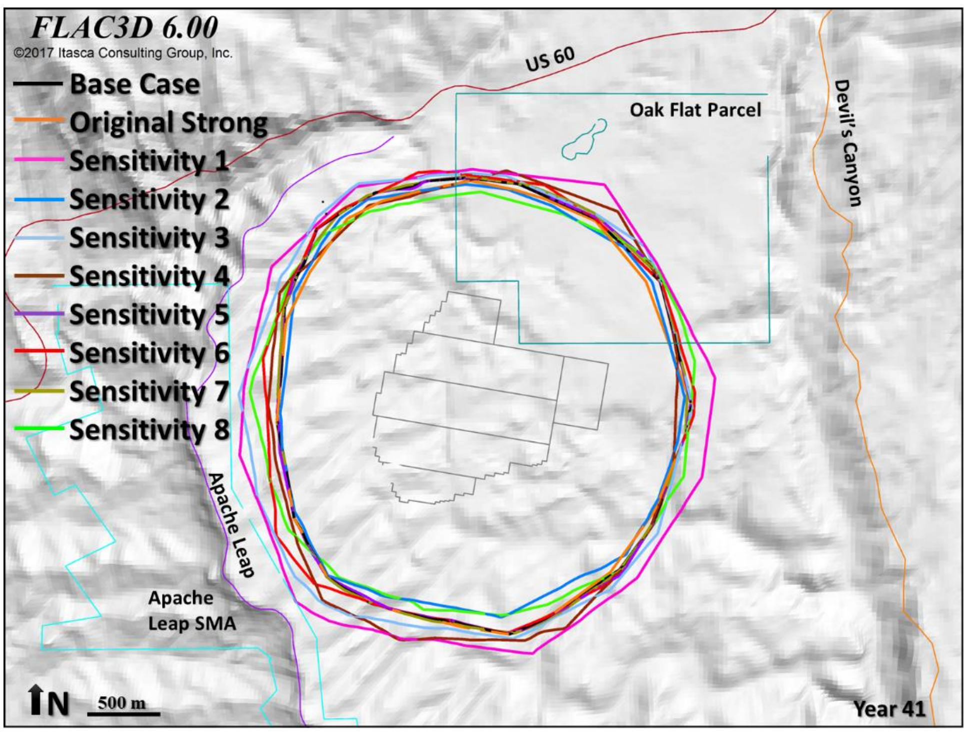

Figure 11 Comparison of predicted fracture limits for base case and all sensitivities.

Table 6 Impact of Sensitivities on Breakthrough Timing and Maximum Crater Depth at End of Mine Life

Model name	Breakthrough Timing	Crater Depth [m]
Base Case	Year 6	240
Original Strong	Year 6	340
Sensitivity 1	Year 7	240
Sensitivity 2	Year 6	240
Sensitivity 3	Year 7	240
Sensitivity 4	Year 6	280
Sensitivity 5	Year 6	260
Sensitivity 6	Year 7	240
Sensitivity 7	Year 6	240
Sensitivity 8	Year 6	240

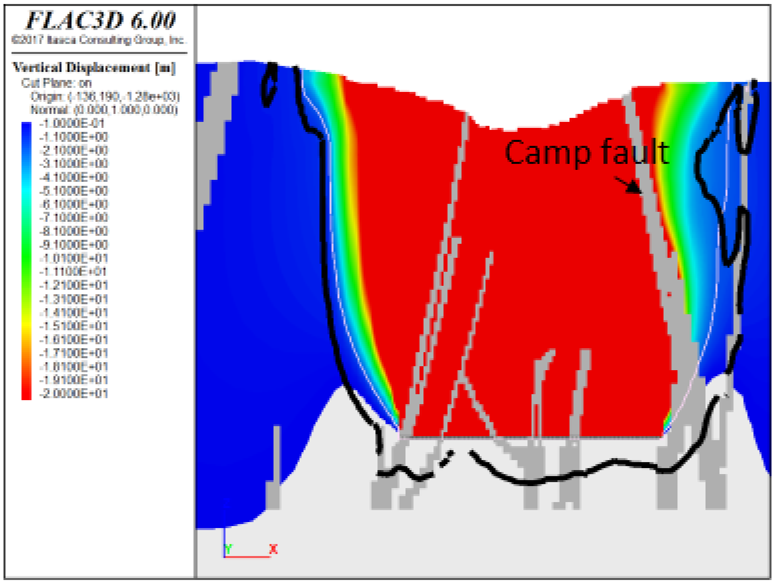

(a)

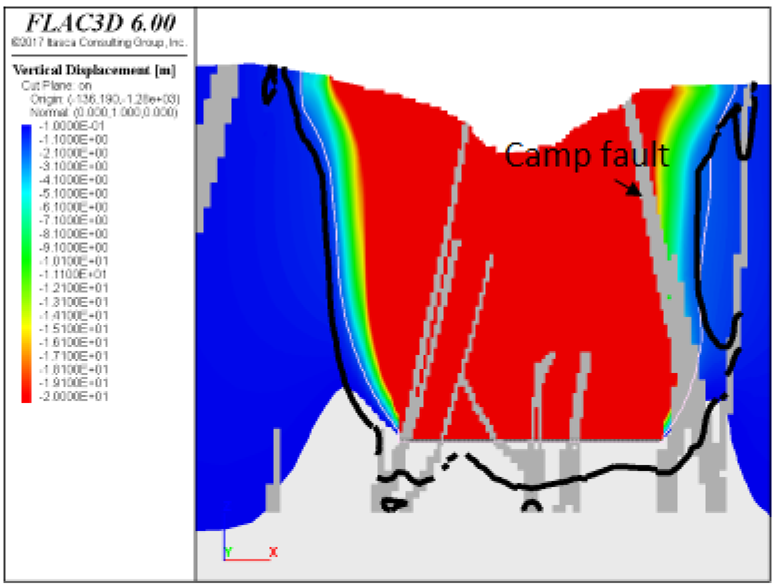

(b)

Figure 12 ***Role of strengthened Camp fault in deepening crater (b) compared to base case (a) by end of mine life.***

4.0 REFERENCES

Hoek, E., C. Carranza-Torres and B. Corkum (2002) "Hoek-Brown failure criterion-2002 edition," *Proceedings of NARMS-Tac*, *1*, pp.267-273.

Li, A. J., et al. (2012) "Parametric Monte Carlo studies of rock slopes based on the Hoek–Brown failure criterion." *Computers and Geotechnics*, 45 pp. 11-18.

Pierce, M. (2010). "Bingham Canyon Mine Cornerstone Feasibility Report"

Rafiei Renani, H., C. Derek Martin, P. Varona and L. Lorig. "Probabilistic stability analysis of slopes in highly heterogeneous rock masses," In preperation.

Sari, M., C. Karpuz, and C. Ayday. (2010) "Estimating rock mass properties using Monte Carlo simulation: Ankara andesites." *Computers & Geosciences*, 36.7 pp. 959-969.

Sharrock, G. (2009) "Investigation of Swell Factors in Block Caving," University of New South Wales, Report to Rio Tinto Technology and Innovation, Report Number RM05186 – DRAFT:1.6. Sydney, Australia.

5.0 APPENDIX A

ITASCA™

SENSITIVITY STUDY OF MODEL PARAMETERS IN THE CAVING PREDICTIONS FOR RESOLUTION COPPER MINE

MINE PLAN OF OPERATIONS

Tryana Garza-Cruz and Matt Pierce

Geometry and Production

- Extraction level depth ~1900m
- Blind orebody with max. column heights ~500m

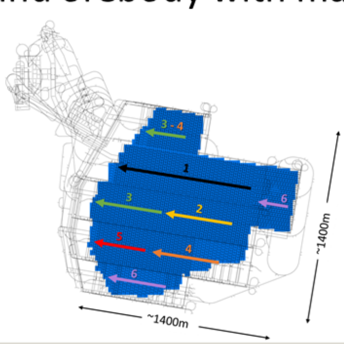

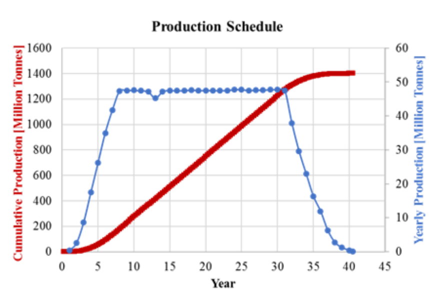

ITASCA™

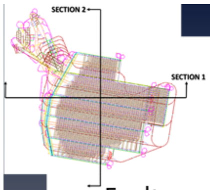

Rock Mass Properties

- Faults modeled implicitly
- Geological units defined based on provided DXFs
- Geotechnical properties from *RCML GTC 2016_0202 Material Properties for Microblock Modeling.docx*

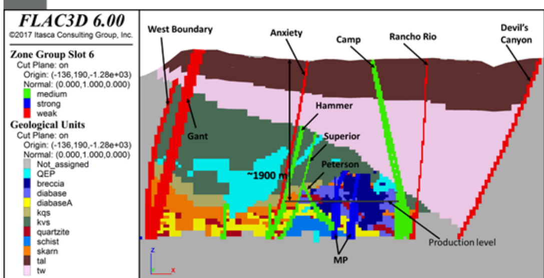

Spatial distribution of lithology on an east-west cross-section (section 1) looking north

Unit	Data				3D Model Parameters			Peak Strength		
	GSI	σ_d (MPa)	m_d	E_d (GPa)	Density	E_{rm} (Gpa)	v	m_{rm}	s	a
Diabase, Basalt	54	54	12	27	2600	10.4	0.24	2.3	0.0060	0.5
Diabase with anhydrite	62	106	15	40	2600	22.6	0.23	3.9	0.0147	0.5
Breccia, QEP	54	55	15	31	2600	12.0	0.24	2.9	0.0060	0.5
Quartzite	69	103	21	39	2600	27.8	0.22	6.9	0.0319	0.5
Tal (Apache Leap Tuff)	64	66	30	30	2600	18.0	0.22	8.2	0.0175	0.5
Tw (Whitetail)	73	23	22	10	2600	7.8	0.21	8.3	0.0476	0.5
KVS, KQS	66	46	30	30	2600	19.3	0.22	8.8	0.0217	0.5
Skarn	63	59	22	40	2600	23.1	0.23	5.8	0.0155	0.5

Rock Mass Strength

- σ_{cm} is the unconfined compressive strength defined by a Mohr-Coulomb fit to the Hoek-Brown curve over a range of confinement from 0 to 25% of the laboratory intact UCS.
- In order to simplify the process of equally varying the rock-mass global-strength (a function of both GSI and UCS) of all units, a relationship between the effect of equally varying both the GSI and UCS to obtain the resulting global strength was generated

ITASCA™

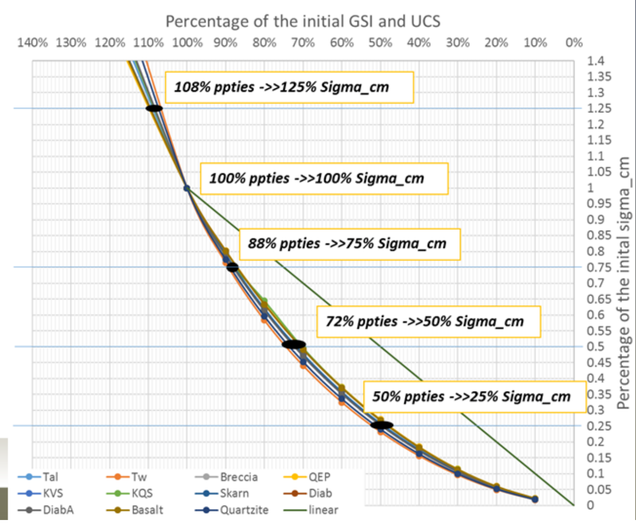

Fault Ranking

- Faults were classified as strong moderate or weak based on description provided by Resolution
  - Strongly annealed faults (strong)
  - Mixed or moderately annealed faults (moderate)
  - Slickensided and/or gouge (weak)

Strong (75% σ_{cm})	Moderate (50% σ_{cm})	Weak (residual prop)
Manske	Andesite	326 Pump Station
Monarch	Camp	Anxiety
MP-1	Hammer N	Concentrator
MP-2	Hammer S	Conley Spring
MP-3	Hammer SW	Devils Canyon
South Boundary	Intergraben	Gant E
	North Boundary A	Gant W
	North Boundary B	Main
	North Boundary C	North Boundary
	Paul	Rancho Rio
	Paul S	West Boundary
	Peterson	
	Superior	
	Superior A	

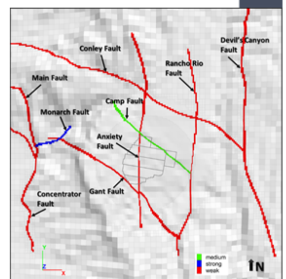

	Base Case	Strong Case	Weak Case
Strong Faults	75% σ_{cm}	88% σ_{cm}	50% σ_{cm}
Medium Faults	50% σ_{cm}	72% σ_{cm}	25% σ_{cm}
Weak Faults	Cohesion = 0, tensile strength = 0, friction = 35°	Cohesion = 0, tensile strength = 0, friction = 35°	Cohesion = 0, tensile strength = 0, friction = 25°

ITASCA™

In-situ Stress

	Base Case	Sensitivity Study	
Principal Stress	Magnitude	75% K0	125% K0
σ_V	25.5*z [km]	25.5*z [km]	25.5*z [km]
σ_H	20.4*z [km]	15.3*z [km]	25.5*z [km]
σ_h	12.75*z [km]	9.56*z [km]	15.94*z [km]

- Base case: σ_H is set N-S

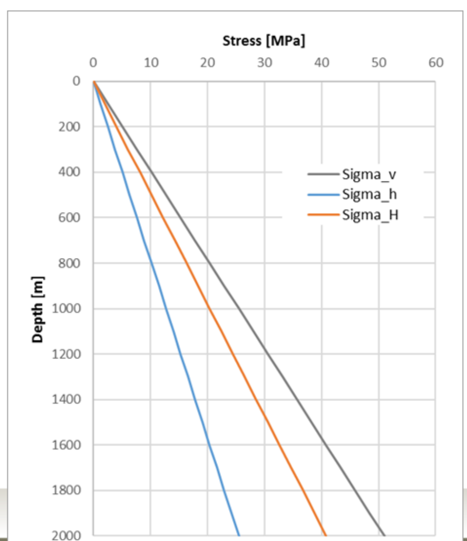

ITASCA™

Cases Examined

Model name	Rock Global Strength	Fault Properties	Residual Strength	Max. VSI	In-situ Stress	Sigma_H direction
Base Case	100%	Base Case	Base Case	0.67 (40% porosity)	Base Case	N-S
Original Strong	100%	Strong Case	Base Case	0.67 (40% porosity)	Base Case	N-S
Sensitivity 1	75% σ_{cm}	Base Case	Base Case	0.67 (40% porosity)	Base Case	N-S
Sensitivity 2	125% σ_{cm}	Base Case	Base Case	0.67 (40% porosity)	Base Case	N-S
Sensitivity 3	100%	Weak Case	Base Case	0.67 (40% porosity)	Base Case	N-S
Sensitivity 4	100%	Base Case	Sensitivity	0.67 (40% porosity)	Base Case	N-S
Sensitivity 5	100%	Base Case	Base Case	0.5 (30% porosity)	Base Case	N-S
Sensitivity 6	100%	Base Case	Base Case	0.67 (40% porosity)	125% K0	N-S
Sensitivity 7	100%	Base Case	Base Case	0.67 (40% porosity)	75% K0	N-S
Sensitivity 8	100%	Base Case	Base Case	0.67 (40% porosity)	Base Case	E-W

Fault Properties

	Base Case	Strong Case	Weak Case
Strong Faults	75% σ_{cm}	88% σ_{cm}	50% σ_{cm}
Medium Faults	50% σ_{cm}	72% σ_{cm}	25% σ_{cm}
Weak Faults	Cohesion = 0, tensile strength = 0, friction = 35°	Cohesion = 0, tensile strength = 0, friction = 35°	Cohesion = 0, tensile strength = 0, friction = 25°

Residual Strength

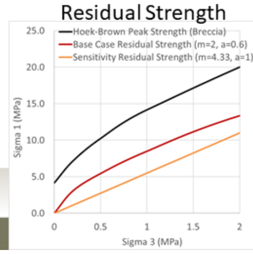

In-situ stress

	Base Case	Sensitivity Study	
Principal Stress	Magnitude	75% K0	125% K0
σ_V	25.5*z [km]	25.5*z [km]	25.5*z [km]
σ_H	20.4*z [km]	15.3*z [km]	25.5*z [km]
σ_h	12.75*z [km]	9.56*z [km]	15.94*z [km]

Angular Distortion

Base Case

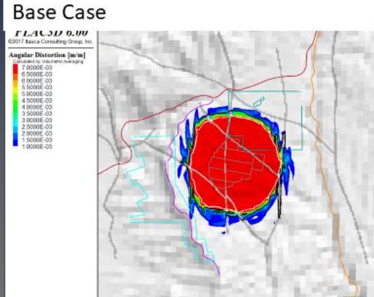

Sensitivity 1 – 75% σcm

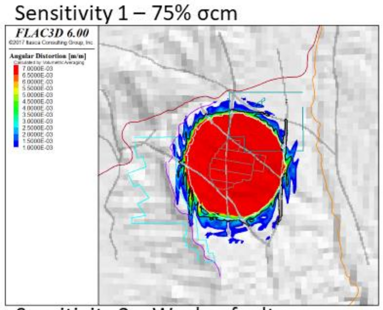

Sensitivity 2 – 125% σcm

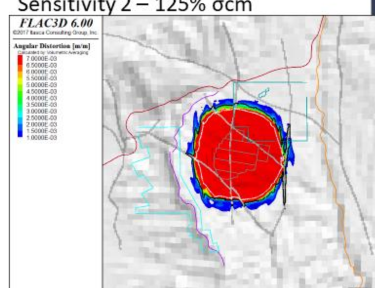

Original Strong

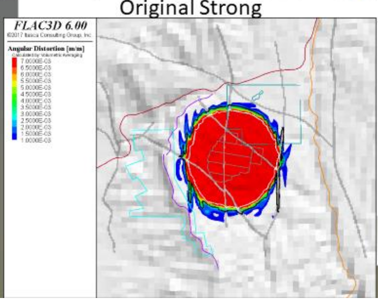

Sensitivity 3 – Weaker faults

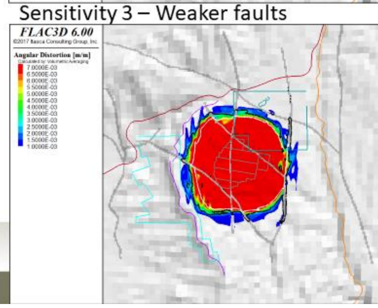

Sensitivity 4 – Lower Residual Strength

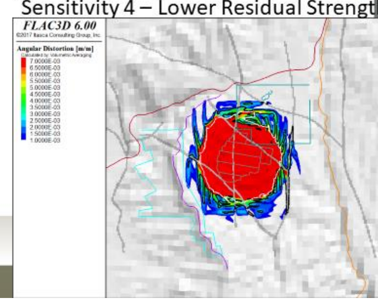

Angular Distortion

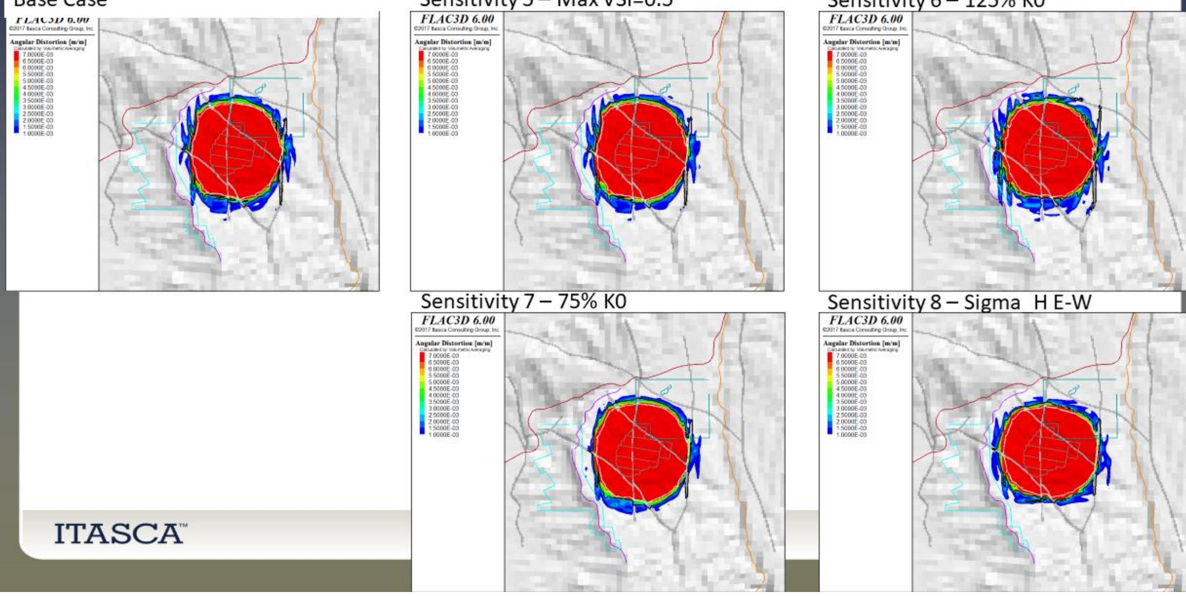

ITASCA

Break-through Timing and Crater Depth

Model name	Break-through timing	Crater Depth [m]
Base Case	Year 6	240
Original Strong	Year 6	340
Sensitivity 1	Year 7	240
Sensitivity 2	Year 6	240
Sensitivity 3	Year 7	240
Sensitivity 4	Year 6	280
Sensitivity 5	Year 6	260
Sensitivity 6	Year 7	240
Sensitivity 7	Year 6	240
Sensitivity 8	Year 6	240

Break-through timing in all cases happens between Year 6-7
Crater depth is influenced by the Camp Fault, which acts to limit the cave boundary relative to the base case when strengthened

ITASCA

Sensitivity to Rock Mass Global Strength

Model name	Rock Global Strength	Fault Properties	Residual Strength	Max. VSI	In-situ Stress	Sigma_H direction
Base Case	100%	Base Case	Base Case	0.67 (40% porosity)	Base Case	N-S
Sensitivity 1	**75% σ_{cm}**	Base Case	Base Case	0.67 (40% porosity)	Base Case	N-S
Sensitivity 2	**125% σ_{cm}**	Base Case	Base Case	0.67 (40% porosity)	Base Case	N-S

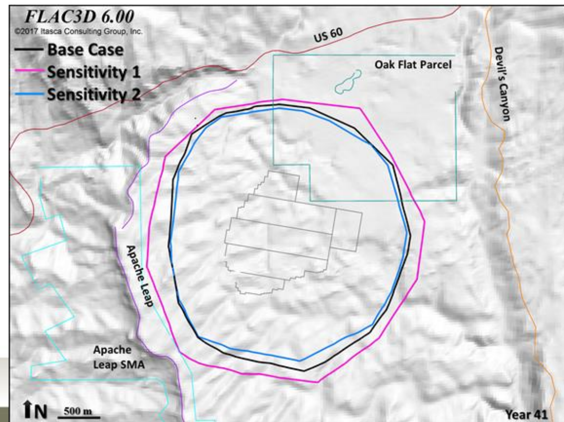

A weaker rock mass sensitivity model also means that faults become weaker than base case

Weaker rock mass global strength extends the fracture limit farther out

ITASCA

Rock Mass Global Strength

- **How conservative are the base case and lower bound rock mass strengths examined?**
- We can understand the range in rock mass strength by performing a Monte Carlo analysis of σ_{cm}
  - Monte Carlo is a well-established technique for understanding rock mass strength distribution
  - Involves randomly sampling the input distributions of GSI and UCS to calculate a distribution of rock mass strength from the Hoek-Brown criterion
  - Example applications:
    - Hoek, Evert. "Reliability of Hoek-Brown estimates of rock mass properties and their impact on design." International Journal of Rock Mechanics and Mining Sciences 35.1 (1998): 63-68.
    - Li, A. J., et al. "Parametric Monte Carlo studies of rock slopes based on the Hoek–Brown failure criterion." Computers and Geotechnics 45 (2012): 11-18.
    - Sari, Mehmet, Celal Karpuz, and Can Ayday. "Estimating rock mass properties using Monte Carlo simulation: Ankara andesites." Computers & Geosciences 36.7 (2010): 959-969.

ITASCA

Rock Mass Global Strength: UCS Distribution

- UCS derived from Point Load data:
  - most complete intact strength data set (227 samples for Apache Leap Tuff)
  - need to multiply by 80% for scale effect

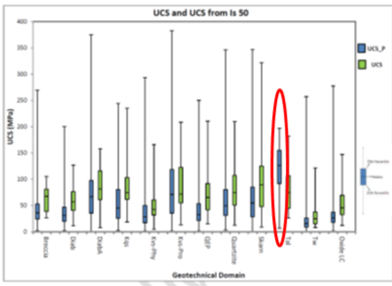

Figure 1-16 Point Loads Vs UCS for each geotechnical domains

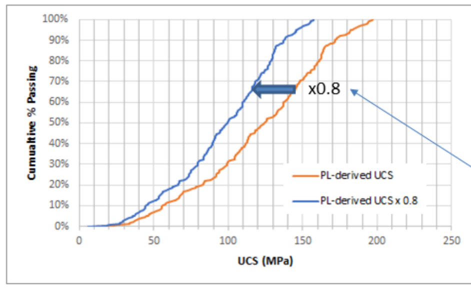

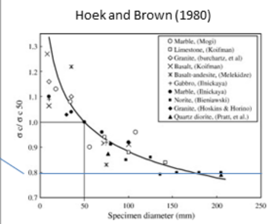

ITASCA

Rock Mass Global Strength: GSI Distribution

- The Geological Strength Index (GSI) was estimated based on block volume using the methodology proposed by Cai et al. (2004).
- Block volumes were estimated from core logging using both apparent spacing and the Joint Weighted Density methodology (Palmstrom, 2005).
  - They give very similar results
  - JWD-derived GSI used

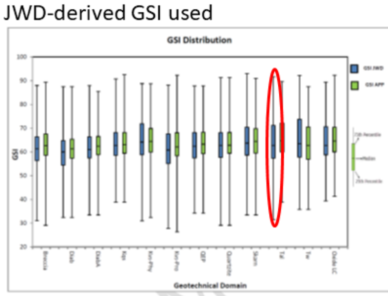

Figure 1-21 Distribution of GSI values for each geotechnical domain (block volume estimated from apparent joint spacing)

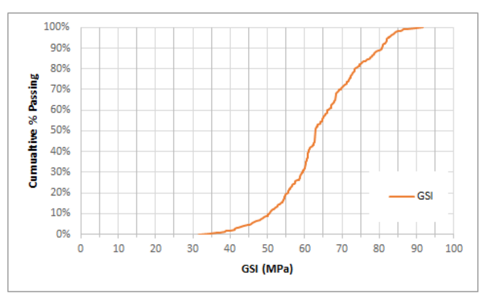

ITASCA

Rock Mass Strength: Monte Carlo Analysis

- UCS and GSI distributions sampled randomly and independently 5000 times (assumes no correlation between UCS and GSI)
- Sigcm (rock mass strength) calculated from each UCS-GSI pair
- Resulting distribution in sigcm reflects variability in rock mass strength at a much smaller scale than the cave
- Representative "controlling" strength in heterogenous materials is typically the 30-40th percentile (Pierce, 2010; Lorig et al., 2018)
- **Base case: 27th percentile (Sigcm=26.0 MPa)**
- **Lower-bound sensitivity: 15th percentile (Sigcm 19.5 MPa)**
  - **Very conservative**

Estimated Range in Rock Mass Strength (sigcm) for Apache Leap Tuff

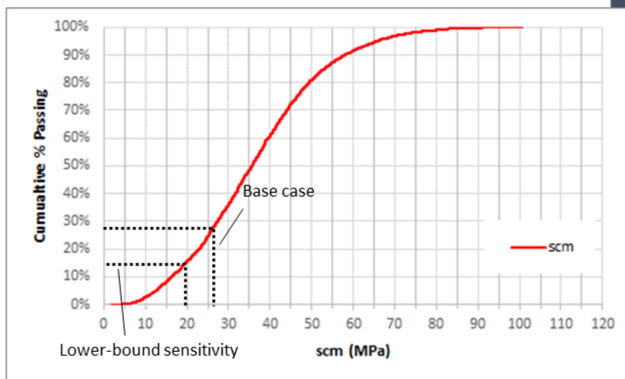

ITASCA™

Sensitivity to Fault Strength

Model name	Rock Global Strength	Fault Properties	Residual Strength	Max. VSI	In-situ Stress	Sigma_H direction
Base Case	100%	Base Case	Base Case	0.67 (40% porosity)	Base Case	N-S
Original Strong	100%	**Strong Case**	Base Case	0.67 (40% porosity)	Base Case	N-S
Sensitivity 3	100%	**Weak Case**	Base Case	0.67 (40% porosity)	Base Case	N-S

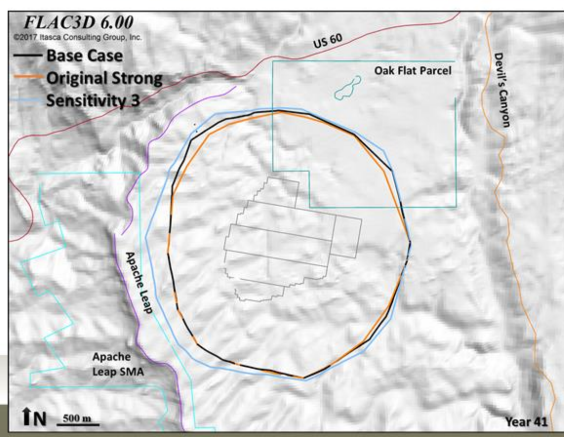

Fault strength has small effect on fracture limit extension

Western expansion in sensitivity 3 case is due to Gantt fault

ITASCA™

Sensitivity to Rock Mass Residual Strength

Model name	Rock Global Strength	Fault Properties	Residual Strength	Max. VSI	In-situ Stress	Sigma_H direction
Base Case	100%	Base Case	Base Case	0.67 (40% porosity)	Base Case	N-S
Sensitivity 4	100%	Base Case	**Sensitivity**	0.67 (40% porosity)	Base Case	N-S

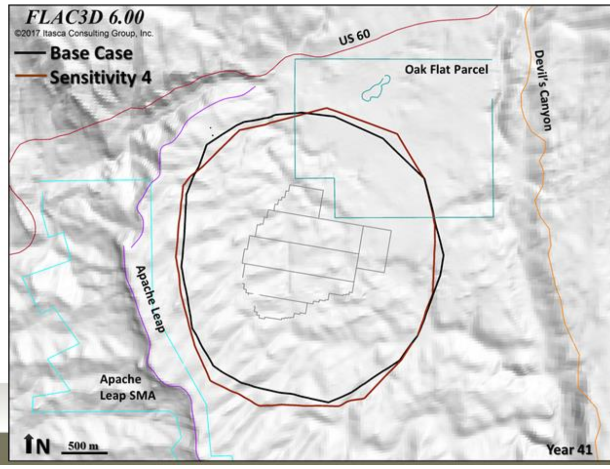

Lower rock mass residual strength slightly reduces the fracture limit extension

Sensitivity to Maximum VSI (Max. Porosity)

Model name	Rock Global Strength	Fault Properties	Residual Strength	Max. VSI	In-situ Stress	Sigma_H direction
Base Case	100%	Base Case	Base Case	0.67 (40% porosity)	Base Case	N-S
Sensitivity 5	100%	Base Case	Base Case	**0.5 (30% porosity)**	Base Case	N-S

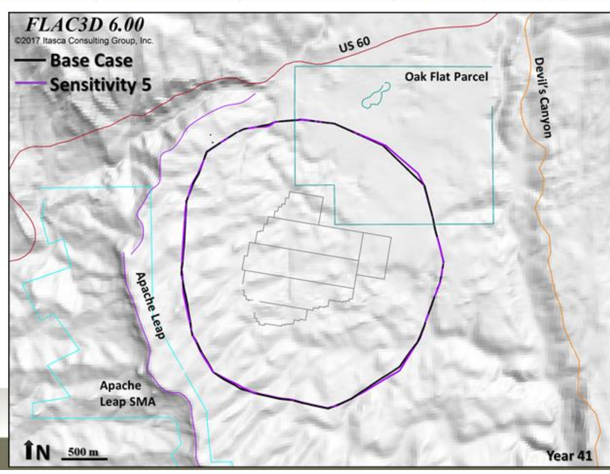

Maximum VSI does not affect fracture limit (sensitive to draw schedule)

Sensitivity to In-situ Stress Magnitude

Model name	Rock Global Strength	Fault Properties	Residual Strength	Max. VSI	In-situ Stress	Sigma_H direction
Base Case	100%	Base Case	Base Case	0.67 (40% porosity)	Base Case	N-S
Sensitivity 6	100%	Base Case	Base Case	0.67 (40% porosity)	**125% K0**	N-S
Sensitivity 7	100%	Base Case	Base Case	0.67 (40% porosity)	**75% K0**	N-S

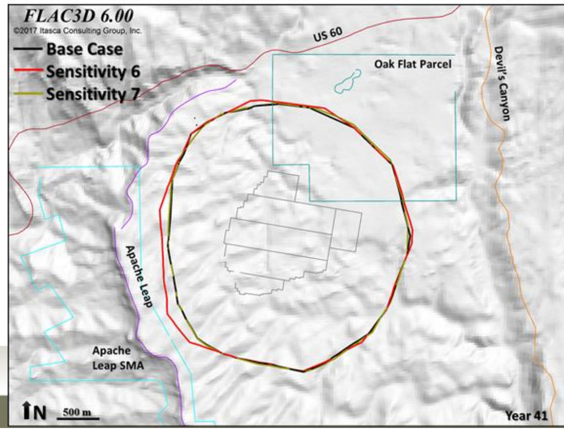

A variation of ±25% of in-situ horizontal stress magnitude has minimal effect on fracture limit

ITASCA™

Sensitivity to Sigma_H Direction

Model name	Rock Global Strength	Fault Properties	Residual Strength	Max. VSI	In-situ Stress	Sigma_H direction
Base Case	100%	Base Case	Base Case	0.67 (40% porosity)	Base Case	N-S
Sensitivity 8	100%	Base Case	Base Case	0.67 (40% porosity)	Base Case	**E-W**

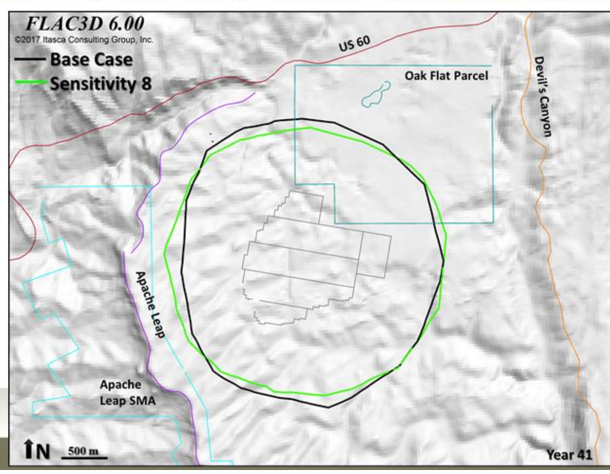

A 90° rotation on in-situ stress direction causes a rotation on the long axis of the fracture limit (E-W)

ITASCA™

All Sensitivities

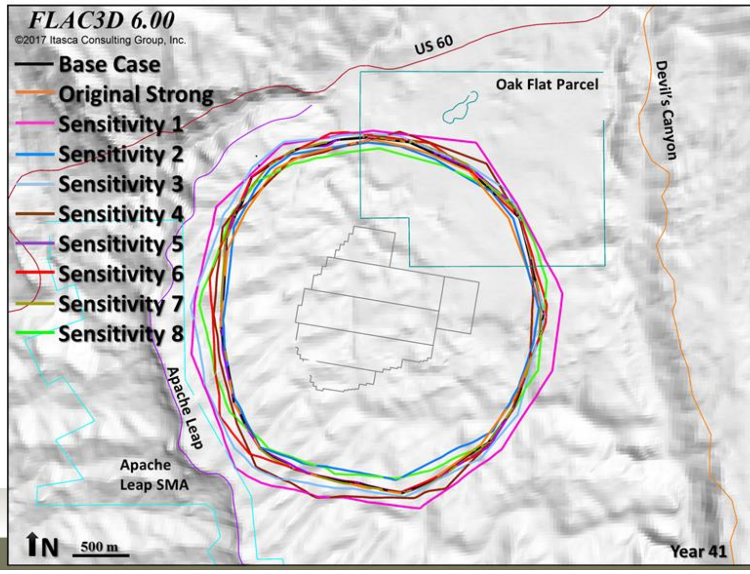

ITASCA

Observations

The sensitivity study revealed:

- **In all cases, no damage to the Apache Leap, Devil's Canyon or to the serviceability of Highway US-60 is expected**
- Fault strength has small effect on fracture limit extension
- Weaker rock mass global strength slightly extends the fracture limit
- Lower rock mass residual strength slightly reduces the fracture limit extension
- Maximum VSI does not affect fracture limit (sensitive to draw schedule)
- A variation of ±25% of in-situ horizontal stress magnitude has minimal effect on fracture limit
- A 90° rotation on in-situ stress direction causes a rotation on the long axis of the fracture limit (E-W)
- Little variability in cave break-through timing (Year 6-7) is observed between cases
- Variability in crater depth is partly due to mesh refinement at deeper levels
- In general, the fracture limits are mainly dependent on the extraction level geometry, depth and draw schedule

ITASCA

102 Magma Heights – P.O. Box 1944
Superior, AZ 85173
Tel.: 520.689.9374
Fax: 520.689.9304

April 10, 2018

Ms. Mary Rasmussen
US Forest Service
Supervisor's Office
2324 East McDowell Road
Phoenix, AZ 85006-2496

Subject: Subsidence Impact Analysis Sensitivity Study

Dear Ms. Rasmussen,

As a follow-up to the geological working group meeting on March 16, 2018 and Resolution Copper's January 9, 2018 letter responding to Baseline Data Request #4, item A1 please see the attached Subsidence Impact Analysis Sensitivity Study.

Should you have any questions or require further information please contact me.

Sincerely,

Vicky Peacey

Vicky Peacey,

Senior Manager, Permitting and Approvals; Resolution Copper Company, as Manager of Resolution Copper Mining, LLC

Cc: Ms. Mary Morissette; Senior Environmental Specialist; Resolution Copper Company

Enclosures:

Itasca Consulting Group Inc.: Subsidence Impact Analysis – Sensitivity Study, Addendum to Itasca Report "*Assessment of Surface Subsidence Associated with Caving*"